

Spring 5-12-2013

Dikar-Induced Synthetic Lethality in a Drosophila Model of CAG Repeat Diseases Does Not Result from an Expression Feedback Loop

Daniel Camacho

University of Connecticut - Storrs, danielcamacho13@hotmail.com

Follow this and additional works at: https://opencommons.uconn.edu/srhonors_theses

 Part of the [Cell Biology Commons](#), and the [Molecular Biology Commons](#)

Recommended Citation

Camacho, Daniel, "Dikar-Induced Synthetic Lethality in a Drosophila Model of CAG Repeat Diseases Does Not Result from an Expression Feedback Loop" (2013). *Honors Scholar Theses*. 295.

https://opencommons.uconn.edu/srhonors_theses/295

HONORS THESIS

DIKAR-INDUCED SYNTHETIC LETHALITY IN A *DROSOPHILA* MODEL OF CAG REPEAT DISEASES DOES NOT RESULT FROM AN EXPRESSION FEEDBACK LOOP

Presented by
Daniel R. Camacho

Department of Molecular and Cell Biology

The University of Connecticut

2013

Abstract

Human CAG repeat diseases manifest themselves through the common pathology of neurodegeneration. This pathological link is attributed to the property shared by all nine of these diseases: an expanded polyglutamine (polyQ) tract. The most evident result of polyQ expansion is protein aggregation, and it is believed that this phenomenon is partly responsible for conferring cytotoxic properties on the mutated protein. Apart from sequestering the mutated protein, cellular aggregates are able to incorporate native proteins via polyQ-mediated aggregation, thus disrupting important cellular pathways. Using *Drosophila melanogaster* as a disease model, researchers have been able to compile collections of these so-called disease modifiers for most of the CAG repeat diseases. Moreover, a recently characterized *Drosophila* gene, *Dikar*, appears to synergistically react with polyQ-expanded proteins in an especially strong fashion, causing a synthetic lethal phenotype. One potential mechanism by which *Dikar* causes synthetic lethality involves the genetic construct used to achieve ectopic gene expression: the *Gal4-UAS* system in conjunction with the *Drosophila* eye-specific transcription factor *Glass* and its enhancer sequence GMR. A suspected chromatin remodelling complex, *Dikar* may create a feedback loop involving GMR that would result in increased polyQ expression and thus cell death. To test whether this phenomenon was responsible for synthetic lethality, a (GFP) reporter gene assay was carried out using two versions of GMR: *longGMR* and *shortGMR*. The findings of this study demonstrated that *Dikar* did not affect GMR-driven expression levels of the GFP reporter. Therefore, it was concluded that synthetic lethality is not the result of a self-perpetuating circuit but rather involves either direct or indirect interactions between *Dikar* and the polyQ protein.

Acknowledgements

I would like to thank the following institutions and individuals: the UCONN Honors Program for enhancing my undergraduate education; the UCONN Department of Molecular & Cell Biology for providing me access to world-class faculty and laboratories; the Rowe Scholars Program and the Presidential Scholars Program for granting me financial support for my research; Dr. Ranyelle Craig for mentoring and introducing me to the world of molecular biology research; Dr. Craig Nelson for advising and inspiring me; and, most important, Dr. Ping Zhang for being a great teacher, mentor, and friend.

Table of Contents

List of Tables	5
List of Figures	6
Introduction	7
Materials and Methods	13
Results	15
Discussion	19
Literature Cited	22

List of Tables

Table 1. Average photon intensity values & statistical analysis data.....	24
--	----

List of Figures

Figure 1. Hypothetical <i>Dikar</i> expression feedback loop	25
Figure 2. Genetic design to generate experimental genotypes	26
Figure 3. Representative fluorescence microscopy images of larval eye disc structures	27
Figure 4. <i>longGMR</i> vs. <i>shortGMR</i> -driven expression of GFP reporter	28

Introduction

CAG repeat expansion mutations are a type of genetic aberration responsible for nine human neurodegenerative diseases, including X-linked spinobulbar muscular atrophy, a series of cerebellar atrophies, and Huntington's disease.¹ In these diseases, native regions of CAG repeats become expanded within the protein-coding regions of affected genes; as a result, the mutation is manifested in the protein products as an expanded stretch of glutamine residues.² The mechanism(s) by which native polyglutamine (polyQ) sequences become expanded remain unclear. One hypothesis postulates that during the processes of DNA replication and/or DNA repair, a phenomenon termed *strand slippage* occurs in the relatively unstable polyQ region of the gene, with the result of increasing the number of CAG trinucleotide units.³ While numerous genes possess native polyQ sequences, the length of these structures remains stable at ~30Q; an increase to 35Q will become a risk factor for disease while expansions beyond 40Q will almost certainly lead to a disease phenotype.⁴ Moreover, the number of CAG copies is correlated both with the severity of the disease as well as the age of onset, with longer polyQ stretches being more detrimental.^{2,4} In terms of inheritance, CAG repeat diseases are autosomal dominant; physiologically, the expanded polyglutamine stretch leads to a dual loss-of-function and gain-of-function mutation of affected genes.⁵

Despite their occurrence among different genes located throughout distinct areas of the genome, CAG repeat mutations result in common pathological manifestations. Mainly, all polyQ expansion-induced diseases are characterized by a senescence of the central nervous system and its associated structures.⁶ In Huntington's disease, the affected gene is responsible for the production of the huntingtin protein.⁷ Normal

huntingtin is expressed ubiquitously in humans and is present at higher levels in the neurons of the CNS, especially in the brain striatum.⁵ Crucially, neuronal cells exhibit increased sensitivity to the polyQ-mutated form of huntingtin (mHtt), with research demonstrating that neurons die from cytoplasmic mHtt concentrations that do not significantly disrupt the functions of other cell types.⁸ This phenomenon has also been observed in other CAG repeat diseases; consequently, the disease phenotypes are the direct result of gradual brain atrophy. The symptoms of CAG repeat-induced neurodegeneration, while varied across the individual diseases, include motor function impairment, psychological alterations, and cognitive decline, with all nine diseases resulting in either symptoms development or even death at approximately the fifth decade of life.⁹

Due to the phenotypic similarities of CAG repeat diseases, it is clear that the expanded polyQ region plays a crucial role in initiating pathological processes. Indeed, this novel structure significantly alters the physiological properties of the affected protein. Most importantly, the expanded polyQ stretch confers aggregating capabilities on the mutated protein, leading to the gain-of-function aspect of the mutation. Depending on the size of the expanded polyQ stretch, mutants will exhibit significant β -structure and/or protofibril characteristics.¹⁰ These structural changes are responsible for aberrant protein folding that leads to protein aggregation at the molecular level as well as inclusion, or aggresome, formation at the microscopic level. Interestingly, polyQ-mutated proteins do not appear to be capable of inducing conformational changes that lead to aggregation of wild-type protein.¹¹ Thus, the presence of an expanded polyQ region is necessary for this phenomenon to take place.

The role of aggregation in disease development is currently a point of debate. Due to the phenotypic similarities of CAG repeat diseases to other neurodegenerative diseases that exhibit amyloid-like protein inclusions, it has been proposed that the molecular event of aggregation is a critical milestone that leads to the development of polyQ-mutated protein cytotoxicity.¹² Moreover, the fact that the length of the mutated polyQ region is related both to enhanced aggregation capabilities as well as the severity of pathology suggests that aggregation contributes significantly to disease development. Not only do aggregates sequester the mutated protein, leading to the loss-of-function aspect of the mutation, but they also are able to recruit other native proteins that contain wild-type polyQ stretches.^{13,14} Thus, aggregation has the potential to disrupt vital cellular pathways.

Nevertheless, the role of inclusions, or aggresomes, in the disease process has been suggested to be beneficial. On the one hand, aggresomes seem to be a final result of the molecular phenomenon of aggregation, indicating that cellular mechanisms have proven incapable of coping with the accumulation of misfolded protein. On the other hand, evidence suggests that aggresomes provide a microenvironment that reduces the concentration of the more toxic monomeric form of the polyQ-mutated protein.¹⁵ Moreover, Taylor et al. found aggresomes display significant chaperone, proteasome, and autophagy activity, and that they allow for an enhanced turnover of aggregated polyQ-mutated protein.¹⁶ Therefore, aggresomes could enable the cell to more effectively target its response pathways.

The ability of inclusions to enter the nucleus is a hallmark of CAG repeat diseases. Yang et al. found that whereas cytoplasmic inclusions localized in the perinuclear region enhanced cell survival, inclusions within the nucleus exhibited a high

degree of toxicity.¹⁷ This group synthesized aggregates of polyQ protein *in vitro* and introduced them into cultured neuronal cell nuclei by engineering a nuclear localization signal (NLS) as part of the protein. Their findings suggest the formation of nuclear inclusions is an important factor that influences aggregate cytotoxicity despite the existence of cytoplasmic inclusions, which had little impact on cell survival. An explanation for this dichotomy is that numerous transcription factors possess polyQ regions that enable these proteins to be incorporated into nuclear inclusions via polyQ-mediated aggregation, with potentially detrimental effects on the regulation of gene expression.¹⁸⁻²⁰ Thus, understanding the interactions between polyQ-mutated protein aggregates and native proteins such as those present in the nucleus is crucial to building a more complete model of polyQ-induced pathology.

To advance this aim, various model systems have been used to investigate the genetic dynamics of CAG repeat diseases. In particular, *Drosophila melanogaster* has proven to be well suited for the study of human neurodegenerative diseases. An important application of *Drosophila melanogaster*, as it relates to polyQ-related neurodegeneration, has been its use for elucidating genes that interact with polyQ-mutated proteins to alter the disease phenotype, so-called disease modifiers. Through the use of genetically engineered versions of the *Drosophila* P-element, various groups have carried out genome-wide mutagenesis screens that either up-regulate or down-regulate native *Drosophila* genes in the presence of transgenic polyQ sequences, either the complete human disease gene or simply the polyQ region.²¹⁻²⁵

In the case of up-regulation, expression of target genes has often been limited to the *Drosophila* eye. This has been achieved through the use of the eye-specific

transcription factor *Glass* and its enhancer sequence GMR in conjunction with the yeast-derived *Gal4-UAS* binary system of ectopic gene expression.^{26,27} Limiting this genetic construct's expression nearly exclusively in the eyes gives researchers flexibility to inflict substantive damage on neuronal tissue that can be easily visualized but that will not compromise the life of the organism, since the *Drosophila* eye is not an essential structure for viability.²⁸ However, *Glass*-driven transcription has been demonstrated to take place outside of eye tissues, making it likely that “leaky” expression of those genes under the control of *Gal4-UAS* will occur.²⁹ In over-expressing ectopic polyQ proteins in the eyes, researchers produced morphological alterations that resulted in what is commonly referred to as a “rough” eye phenotype. Through genetic screens, numerous modifiers that alter this rough eye phenotype, either suppressing or enhancing it, have been discovered for several of the CAG repeat diseases, and these findings have been used to explore possible targets for therapeutic approaches.

Until recently, it was believed that genome-wide screens for disease modifiers could be carried out simply by combining a human polyQ protein with the up-regulated *Drosophila* targeted gene in the F₁ generation and looking for changes in the rough eye defect. Nevertheless, Zhang et al. characterized a *Drosophila* gene, *Dikar*, that, when over-expressed in combination with several types of polyQ proteins, displayed synergistic interaction with polyQ proteins that resulted in synthetic lethality.³⁰ Additionally, when overexpressed in the absence of polyQ, *Dikar* itself was able to cause a rough eye-like phenotype. However, unlike polyQ proteins, *Dikar* over-expression at high levels did not cause widespread death. These findings suggest that the current approach used for the screening of disease modifiers in polyQ-induced neurodegeneration

is incapable of detecting the most “reactive” modifiers, since the synthetic lethal phenotype they produce will virtually eliminate any chances of recovering those genotypes containing them in a usual F₁ screen.

The mechanism(s) through which *Dikar* produces synthetic lethality remain unclear. One possibility is related to the presumed cellular function of *Dikar*. Sequence analysis has demonstrated *Dikar* contains an acetyl transferase domain and is the homologue of the human CECR2 gene, a chromatin remodeling complex that is known to activate a set of downstream genes.^{31,32} Because *Dikar* potentially plays a role in the regulation of gene expression, its effect on polyQ cytotoxicity may involve a feedback loop in which overexpression of *Dikar* drives expression of the polyQ protein above experimentally set levels, overwhelming cellular coping mechanisms and resulting in widespread cell death. This self-perpetuating circuit would presumably have its effect within the region of GMR, since this sequence is the link between the expression of *Dikar* and polyQ via the *Gal4-UAS* system (Figure 1). To determine whether this phenomenon is responsible for the synthetic lethal phenotype, a reporter gene assay was conducted using green fluorescent protein (GFP) as a reporter, both in the absence and presence of *Dikar* overexpression.

Materials and Methods

Culture media and Drosophila stocks: Fruit flies were raised using corn/agar media (H₂O, agar, cornmeal, baker's yeast, table sugar, Moldex® dissolved in ethanol) and incubated at 25°C. The following alleles were obtained from the Bloomington *Drosophila* Stock Center: *longGMR-Gal4* (No. 8605), *shortGMR-Gal4* (No. 1104), *UAS-2xEGFP* (No. 6658). The d10135 chromosome, which carries UAS-linked *Dikar*, was obtained from the Berkeley *Drosophila* Genome Project.

Fly dissection and fluorescence microscopy: Third instar larvae were dissected in phosphate buffer (PBS, 130 mM NaCl, 7 mM Na₂HPO₄·2H₂O, 3 mM NaH₂PO₄·2H₂O, pH 7.0) to expose and isolate eye disc structures. Tissues were mounted on slides using cover slips and PBS, and they were immediately visualized using an Olympus microscope. Green fluorescent images of tissues were taken with a digital camera mounted on the microscope (CCD Spot, Diagnostic Instrument, Inc.). Images of 20 different tissue samples were taken at minimum for each of the four genotypes being analyzed.

Image processing and statistical analysis: Digital images taken from fluorescence microscopy were processed using the software ImageJ (The National Institutes of Health). Images were split by color channels, and only the green channel was used for measuring photon intensity. The “region of interest” (ROI) tool of the software was used to draw the borders of the areas to be quantified. Areas chosen were those that displayed intermediate intensities relative to all the signals detected for a given image. The mean

intensity values of the designated areas were quantified by the software within a 0-255 range. These values were used to construct data sets for each of the four genotypes being analyzed. Using the “Analysis ToolPack” add-in of Excel (2011 version), the data sets for the control and experimental groups were statistically analyzed using the “t-Test: Two-Sample Assuming Unequal Variances” setting in order to generate p values. The data set for genotype *+/+ ; longGMR-Gal4 // + ; UAS-2xEGFP // + ; +/+ (control)* was compared to that of genotype *+/+ ; longGMR-Gal4 // + ; UAS-2xEGFP // UAS-Dikar ; +/+ (experimental)* and the data set for genotype *+/+ ; shortGMR-Gal4 // + ; UAS-2xEGFP // + ; +/+ (control)* was compared to that of genotype *+/+ ; shortGMR-Gal4 // + ; UAS-2xEGFP // UAS-Dikar ; +/+ (experimental)*.

Results

Genetic manipulations to produce control genotypes: Two types of genetic crosses were carried out to generate four genotypes of interest. The first type involved a cross of the following genotypes: (σ) X/Y ; *longGMR-Gal4* / *longGMR-Gal4* ; +/+ ; +/+ X (ρ) X/X ; +/+ ; UAS-2xEGFP / UAS-2xEGFP ; +/+. This cross produced an F₁ generation all containing the following autosomes: *longGMR-Gal4* / + ; UAS-2xEGFP / + ; +/+. Consequently, all members of this generation possessed fluorescence in the eye discs. An analogous sequence was carried out using males carrying the *shortGMR* construct instead of *longGMR*. Therefore, this type of genetic cross produced offspring containing both *GMR-Gal4*, either *shortGMR* or *longGMR*, and UAS-2xEGFP (control).

Genetic manipulations to produce experimental genotypes: The second type of cross involved more complex genetics due to the challenges posed by combining *GMR-Gal4*, *UAS-2xEGFP*, and *UAS-Dikar* together in one genotype (Figure 2). Mainly, homozygotes for *GMR-Gal4* and *UAS-Dikar* are difficult to establish because this genotype is unstable. Therefore, a genotype carrying both of these genetic elements in the heterozygous condition (*GMR-Gal4* on C-2 and *UAS-Dikar* on C-3) had to be designed with the use of balancer chromosomes in order to suppress any recombination that would split the UAS sequence from its downstream target gene. The type of balancer chromosome employed was actually a set of two reciprocally translocated balancer autosomes, represented as T(2;3)CyO-TM6, and they were established in a male line. Due to gene dose imbalance, however, a genotype carrying the translocated chromosomes (e.g. + ; + / T(2;3)CyO-TM6) can only produce two types of viable

gametes: + ; + and T(2;3)CyO-TM6. Given this limitation, it was expected that only 50% of the F₁ generation that resulted from a cross of these males with females used in the control crosses would live; that is, only those organisms carrying viable genetic combinations. Once offspring were generated, there was an additional challenge. Due to the genetic design, only 50% of viable offspring would display eye disc fluorescence. The other 50% would contain the translocated balancer chromosomes in addition to *UAS-2xEGFP*. Normally these two groups would be differentiated easily in the adult form since the balancer chromosome contains a dominant marker: CyO. However, because the experimental design consisted of analyzing larvae, this phenotypic distinction had not yet developed. The means to overcome this limitation was simply to dissect larvae randomly, knowing that each larvae chosen possessed a 50% chance of exhibiting eye disc fluorescence. As was the case for the control, the type of genetic manipulation described above was carried out using the *longGMR-Gal4* construct in one instance and the *shortGMR-Gal4* construct in the other.

shortGMR: 20 images of tissue samples were analyzed for genotype *+/+ ; shortGMR-Gal4 // + ; UAS-2xEGFP // + ; +/+* (Figure 4). Photon intensity data from these images were used to calculate a mean photon intensity value of green fluorescence for this genotype, designated “**sGMR**” (Table 1). This data set displayed the following parameters: mean = 59.706, variance = 221.108. Also, 20 images of tissue samples were analyzed for genotype *+/+ ; shortGMR-Gal4 // + ; UAS-2xEGFP // UAS-Dikar ; +/+* (Figure 4). Mean photon intensity values for these images were used to calculate a mean photon intensity value of green fluorescence for this genotype, designated “**sGMR**

Dikar” (Table 1). This data set displayed the following parameters: mean = 63.541, variance = 152.360. Both data sets were compared, and they generated a p value of 0.168. This indicates there is no statistically significant difference between the two data sets ($p < 0.05$).

longGMR: 22 images of different tissue samples were analyzed for genotype $+/+ ; longGMR-Gal4 // + ; UAS-2xEGFP // + ; +/+$ (Figure 4). Mean photon intensity values for these images were used to calculate a mean photon intensity value of green fluorescence for this genotype, designated “**IGMR**” (Table 1). This data set displayed the following parameters: mean = 7.194, variance = 6.228. Also, 23 images of different tissue samples were analyzed for genotype $+/+ ; longGMR-Gal4 // + ; UAS-2xEGFP // UAS-Dikar ; +/+$ (Figure 4). Mean photon intensity values for these images were used to calculate a mean photon intensity value of green fluorescence for this genotype, designated “**IGMR Dikar**” (Table 1). This data set displayed the following parameters: mean = 7.020, variance = 6.494. Both data sets (IGMR & IGMR Dikar) were compared, and they generated a p value of 0.409. This indicates there is no statistically significant difference between the two data sets ($p < 0.05$).

longGMR vs. shortGMR: Mean photon intensity values between *longGMR* and *shortGMR*-driven expression of GFP reporter were compared (Figure 3). Since genotypes either containing *Dikar* or not were not found to be statistically different, their data sets were combined for the purposes of this comparison. The mean intensity value for *longGMR*-driven expression was 12.79 while that for *shortGMR*-driven expression was

123.25, indicating that *shortGMR*-driven expression is ~9 times greater than *longGMR*-driven expression.

Discussion

The purpose of this investigation was to determine if a feedback expression loop, involving the enhancer sequence GMR and the *Drosophila* protein *Dikar*, was the cause of the synthetic lethality that results from the simultaneous ectopic overexpression of human polyQ-mutated proteins and *Dikar*. Because the phenomenon of synthetic lethality at present is limited to *Dikar* expression, a self-perpetuating circuit is a potential explanation for this supposed isolated observation. Indeed, expression of polyQ proteins at certain levels is sufficient to cause widespread cell death, with a feedback loop resulting in an exact scenario.

The genetic construct used to study CAG repeat diseases in *Drosophila* utilizes various genetic elements (Figure 1). A *Drosophila* eye-predominant transcription factor, *Glass*, along with its enhancer sequence GMR, is used to virtually limit ectopic expression to the eyes. Moreover, the yeast-derived *Gal4-UAS* system is used to drive expression of target genes. These two elements are linked via the *GMR-Gal4* construct, which ultimately combines *Glass*-induced transcription to the expression of genes downstream of UAS sequences. Within this genetic construct, a potential weakness involves the ability of target genes to modulate the dynamics of either *Glass* or the GMR sequence, thereby altering the experimentally pre-determined expression levels of the target genes. In considering *Dikar* and its cellular role in the regulation of gene expression via chromatin remodelling, synthetic lethality can be the result of *Dikar*-induced changes on the GMR sequence, which would lead to increased expression of *Gal4* and thus of the polyQ-containing protein.

A reporter gene assay using green fluorescent protein (GFP) was carried out to determine *Dikar*'s effect on GMR-driven expression of target genes. The experimental design consisted of the following elements. First, two common GMR derivatives were used: *longGMR* (*lGMR*) and *shortGMR* (*sGMR*). The primary differences between these two are: 1) *longGMR* carries more *Glass*-binding sites than *shortGMR* and 2) *shortGMR* achieves greater levels of expression in the eyes than does *longGMR*. Two versions of GMR were used to further validate the experimental findings inasmuch as both GMR sequences yield the same results. Second, 2 types of genotypes were generated for each GMR sequence (4 genotypes of interest in total). One type contained the *GMR-Gal4* and *UAS-2xEGFP* constructs only and served as a control to establish baseline expression of the GMR sequence. The other genotype contained the *GMR-Gal4* and *UAS-2xEGFP* constructs as well as *UAS-Dikar* (Figure 2), and it served to determine *Dikar*'s effect, if any, on the expression of GMR-controlled genetic elements.

GFP reporter expression was measured using fluorescence microscopy. In order to optimize visualization of the green fluorescence signal, eye tissue samples were obtained from third instar larvae. In particular, eye discs, primordial structures of the adult eye, were dissected out and prepared for microscopy. This made for a more efficient means of obtaining appropriate tissues without the need to process tough, adult cuticle. Simultaneous to visualization, tissue samples were imaged using a CCD camera to reduce "background" signals. No qualitative difference was observed between those genotypes possessing the same GMR sequence either in the absence or presence of *Dikar* (Figure 4). Subsequently, images were processed, and this data was used to generate quantitative mean photon intensity values for each of the four genotypes of interest (Table 1).

Statistical analysis of these values demonstrated no significant difference between genotypes possessing the same GMR sequence either in the absence or presence of *Dikar*. Moreover, the difference in reporter expression observed between the *longGMR* and *shortGMR* constructs (Figure 3) reflected the dynamics of these two sequences found in the literature. This outcome validated both the genetic design as well as the experimental findings. Given this data, it was concluded that *Dikar* did not affect GMR-driven expression of the GFP reporter.

Therefore, the experimental results did not support the concept of a *Dikar* expression feedback loop as the causation of polyQ-related synthetic lethality in *Drosophila*. These findings have two major implications. First, a discrediting of the expression feedback loop hypothesis posits a more complex relation between polyQ-mutated proteins and *Dikar*. Based on the experimental results, it is likely that synthetic lethality is the product of either direct or indirect interactions between these two gene products. As such, further research on the mechanism(s) by which *Dikar* causes synthetic lethality is needed. Second, the probability that *Dikar* is the only gene capable of eliciting a “legitimate” synthetic lethal phenotype seems unlikely. Given this assumption, the current approach to finding polyQ disease modifiers in *Drosophila* via genome-wide screens appears to have a major flaw. Simply stated, these screens are unable to recover the most powerful modifiers: those that modify polyQ cytotoxicity to the point of death. Thus, a re-evaluation of this protocol that reflects this reality is necessary for the discovery of genes that may ultimately serve as therapeutic targets for these diseases.

Literature Cited

1. Ross CA, Poirier MA. Protein Aggregation and Neurodegenerative Disease. *Nature Medicine* 10.7: S10-17, 2004.
2. Housman D. Gain of glutamines, gain of function? *Nature Genet* 10: 3-4, 1995
3. Petruska J, Hartenstein MJ, Goodman MF. Analysis of Strand Slippage in DNA Polymerase Expansions of CAG/CTG Triplet Repeats Associated with Neurodegenerative Disease. *Journal of Biological Chemistry* 273: 5204-210, 1998.
4. Brinkman RR, Mezei MM, Theilmann J, Almqvist E, Hayden MR. The likelihood of being affected with Huntington disease by a particular age, for a specific CAG size. *Am J Hum Genet*; 60:1202–1210, 1997.
5. Zuccato C, Valenza M, Cattaneo E. Molecular Mechanisms and Potential Therapeutical Targets in Huntington's Disease. *Physiological Reviews* 90.3: 905-81, 2010.
6. Ross CA. When more is less: pathogenesis of glutamine repeat neurodegenerative diseases. *Neuron* 15: 493-6, 1995
7. Bates GHP, Jones AL. Huntington's Disease. Oxford, UK: Oxford Univ. Press, 2002.
8. Cisbani, G, Cicchetti F. An in Vitro Perspective on the Molecular Mechanisms Underlying Mutant Huntingtin Protein Toxicity. *Cell Death and Disease* 382: n. pag., 2012
9. Rosenblatt A. Neuropsychiatry of Huntington's disease. *Dialogues Clin Neurosci* 9: 191–197, 2007
10. Harjes P, Wanker EE. The hunt for huntingtin function: interaction partners tell many different stories. *Trends Biochem Sci* 28: 425–433, 2003.
11. Zhang Y, Li M, Drozda M, Chen M, Ren S, Mejia Sanchez RO, et al. Depletion of wild-type huntingtin in mouse models of neurologic diseases. *J Neurochem.*; 87:101–106. 2003.
12. Leavitt BR, van Raamsdonk JM, Shehadeh J, Fernandes H, Murphy Z, Graham RK, et al. Wild-type huntingtin protects neurons from excitotoxicity. *J Neurochem.*; 96:1121–1129, 2006.
13. Leavitt BR, van Raamsdonk JM, Shehadeh J, Fernandes H, Murphy Z, Graham RK, et al. Wild-type huntingtin protects neurons from excitotoxicity. *J Neurochem.*; 96:1121–1129, 2006.
14. DiFiglia, M., Sapp, E., Chase, K.O., Davies, S.W., Bates, G.P., Vonsattel, J.P. and Aronin, N. Aggregation of huntingtin in neuronal intranuclear inclusions and dystrophic neurites in brain. *Science*, 277, 1990–1993, 1997.
15. Arrasate M, Mitra S, Schweitzer ES, Segal MR, Finkbeiner S. Inclusion body formation reduces levels of mutant huntingtin and the risk of neuronal death. *Nature.*; 431:805–810, 2001.
16. Taylor JP, Tanaka F, Robitschek J, Sandoval CM, Taye A, Markovic-Plese S, et al. Aggresomes protect cells by enhancing the degradation of toxic polyglutamine-containing protein. *Hum Mol Genet.*; 12:749–757, 2003.
17. Yang W, Dunlap JR, Andrews RB, Wetzel R. Aggregated polyglutamine peptides delivered to nuclei are toxic to mammalian cells. *Hum Mol Genet* 11: 2905–2917, 2002.
18. Nucifora, F.C., Jr., Sasaki, M., Peters, M.F., Huang, H., Cooper, J.K., Yamada, M., Takahashi, H., Tsuji, S., Troncoso, J., Dawson, V.L. et al. (2001) Interference by huntingtin and atrophin-1 with cbp-mediated transcription leading to cellular toxicity. *Science*, 291, 2423–2428.
19. McCampbell, A. and Fischbeck, K.H. (2001) Polyglutamine and CBP: fatal attraction? *Nat. Med.*, 7, 528–530.

20. Okazawa, H., Rich, T., Chang, A., Lin, X., Waragai, M., Kajikawa, M., Enokido, Y., Komuro, A., Kato, S., Shibata, M. et al. (2002) Interaction between mutant ataxin-1 and PQBP-1 affects transcription and cell death. *Neuron*, 34, 701–713
21. P Fernandez-Funez, ML Nino-Rosales, B de Gouyon, WC She, JM Luchak, P Martinez, E Turiegano, J Benito, M Capovilla, PJ Skinner, et al: Identification of genes that modify ataxin-1-induced neurodegeneration. *Nature* 2000, 408:101-6.
22. P Kazemi-Esfarjani, S Benzer: Genetic suppression of polyglutamine toxicity in *Drosophila*. *Science* 2000, 287:1837-40.
23. J Bilén, NM Bonini: Genome-wide screen for modifiers of ataxin-3 neurodegeneration in *Drosophila*. *PLoS Genet* 2007, 3:1950-64.
24. S Zhang, R Binari, R Zhou, N Perrimon: A genomewide RNA interference screen for modifiers of aggregates formation by mutant Huntingtin in *Drosophila*. *Genetics* 2010, 184:1165-79.
25. H Vossfeldt, M Butzlaff, K Prussing, RA Ni Charthaigh, P Karsten, A Lankes, S Hamm, M Simons, B Adryan, JB Schulz, et al: Large-scale screen for modifiers of ataxin-3-derived polyglutamine-induced toxicity in *Drosophila*. *PLoS One* 2012, 7:e47452.
26. Moses, K., G. M. Rubin. Glass Encodes a Site-specific DNA-binding Protein That Is Regulated in Response to Positional Signals in the Developing *Drosophila* Eye. *Genes & Development* 5.4: 583-93, 1994
27. Southall, T. D., D. A. Elliott, and A. H. Brand. The GAL4 System: A Versatile Toolkit for Gene Expression in *Drosophila*. *Cold Spring Harbor Protocols* 2008.8: Pdb.top49, 2008
28. Halder, G., P. Callaerts, S. Flister, U. Walldorf, U. Kloter, and W. J. Gehring. Eyeless Initiates the Expression of Both *Sine Oculis* and *Eyes Absent* during *Drosophila* Compound Eye Development. *Development* 125: 2181-191, 1998
29. MC Ellis, EM O'Neill, GM Rubin: Expression of *Drosophila* glass protein and evidence for negative regulation of its activity in non-neuronal cells by another DNA-binding protein. *Development* 1993, 119:855-65.
30. P. Zhang, Q. Wang, H. Hughes, G. Intrieri, D. Camacho. Synthetic Lethality Induced by Coexpressing the *Drosophila Dikar* Gene and an Expanded Polyglutamine Tract with the *GMR-Gal4/UAS* System. (2013, Manuscript in preparation)
31. Keuling, A., F. Yang, S. Hanna, H. Wang, T. Tully, A. Burnham, J. Locke, and H. McDermid. Mutation Analysis of *Drosophila Dikar/CG32394*, Homologue of the Chromatin-remodelling Gene *CECR2*. *Genome* 50: 767-77, 2007
32. Fairbridge, Nicholas A., Christine E. Dawe, Farshad H. Niri, Megan K. Kooistra, Kirst King-Jones, and Heather E. McDermid. *Cecr2* Mutations Causing Exencephaly Trigger Misregulation of Mesenchymal/ectodermal Transcription Factors. *Birth Defects Research Part A: Clinical and Molecular Teratology* 88.8: 619-25, 2010

<i>Parameters</i>	<i>sGMR</i>	<i>sGMR Dikar</i>	<i>IGMR</i>	<i>IGMR Dikar</i>
Mean	59.706	63.541	7.195	7.020
Variance	221.108	152.360	6.228	6.494
Observations	20.000	20.000	22.000	23.000
Pearson Correlation	0.199	-	6.364	-
Hypothesized Mean Difference	0.000	-	0.000	-
df	19.000	-	43.000	-
t Stat	-0.989	-	0.232	-
P(T<=t) one-tail	0.168	-	0.409	-
t Critical one-tail	1.729	-	1.681	-
P(T<=t) two-tail	0.335	-	0.818	-
t Critical two-tail	2.093	-	2.017	-

Table 1. Average photon intensity values & statistical analysis data. Mean value comparison between data sets of genotypes *sGMR* (59.706) and *sGMR Dikar* (63.541) determined no statistically significant difference between the two (p value = 0.168). Similarly, the comparison between data sets of genotypes *IGMR* (7.195) and *IGMR Dikar* (7.020) determined no statistically significance difference between the two (p value = 0.409). Therefore, expression of *Dikar* does not impact expression of GMR-driven expression (either *longGMR* or *shortGMR*) of GFP reporter.

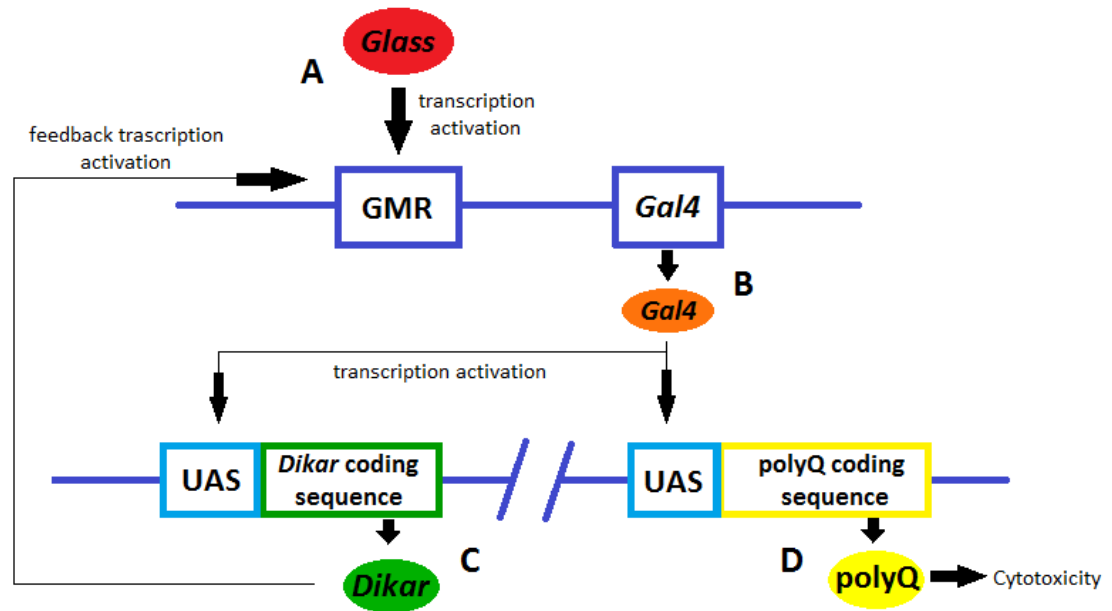


Figure 1. Hypothetical *Dikar* expression feedback loop. A) Eye-predominant transcription factor *Glass* binds to its enhancer sequence, GMR, and drives transcription of *Gal4* gene. B) *Gal4* binds its enhancer sequence, UAS, and activates transcription of downstream genes; in this genetic construct these are the *Drosophila* gene *Dikar* and a human polyQ-containing transgene. C) *Dikar* is able to affect GMR-driven transcription, perhaps through chromatin remodelling, and causes expression of the *Gal4* gene above experimentally-set levels. D) An increased dose of *Gal4* drives increased expression of the polyQ-disease protein, which acts as a cytotoxin and whose level of expression overwhelms cellular coping mechanisms. This self-perpetuating feedback circuit is one supposed mechanism by which *Dikar* expression, in combination with polyQ expression, leads to a synthetic lethal phenotype in *Drosophila*.

P generation males:

$$\frac{GMR-Gal4}{T(2;3) a} ; \frac{UAS-Dikar}{T(2;3) b}$$



Possible genotypes:

A	<i>GMR-Gal4 ; UAS-Dikar</i>	viable
B	<i>T(2;3) a ; T(2;3) b</i>	viable
C	<i>GMR-Gal4 ; T(2;3) b</i>	inviable
D	<i>T(2;3) a ; UAS-Dikar</i>	inviable

P generation:

$$\frac{X}{Y} ; \frac{GMR-Gal4}{T(2;3) a} ; \frac{UAS-Dikar}{T(2;3) b} ; \frac{+}{+} \quad \otimes \quad \frac{X}{X} ; \frac{+}{+} ; \frac{UAS-2xEGFP}{UAS-2xEGFP} ; \frac{+}{+}$$



F₁ possible genotypes:

$$\frac{GMR-Gal4}{+} ; \frac{UAS-Dikar}{UAS-2xEGFP} ; \frac{+}{+} \quad \& \quad \frac{T(2;3) a}{+} ; \frac{T(2;3) b}{UAS-2xEGFP} ; \frac{+}{+}$$

Figure 2. Genetic design to generate experimental genotypes. Top) Males carrying the translocated balancer chromosome *T(2;3) CyO-TM6* (represented as “*T(2;3) a*” & “*T(2;3) b*”) only produced two sets of viable gametes. Bottom) Cross to generate experimental genotypes (**IGMR Dikar** and **sGMR Dikar**) produced two distinct autosomal genotypes in the F₁ generation. Out of these, only the one carrying the *GMR-Gal4* construct displayed green fluorescence in eye discs of larvae.

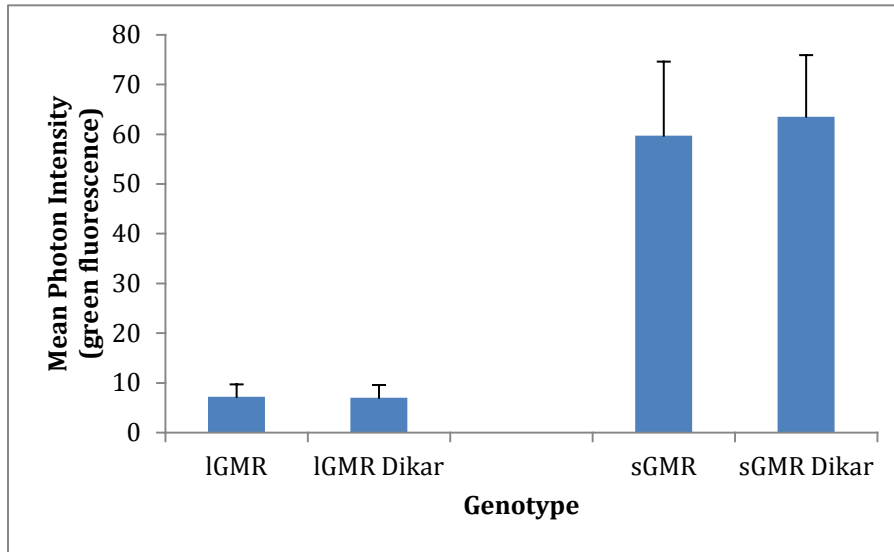


Figure 3. *longGMR* vs. *shortGMR*-driven expression of GFP reporter. Experimental findings presented in Table 1 demonstrated no difference between GMR-driven expression of GFP reporter either in the presence or absence of *Dikar* expression ($p > 0.05$). Therefore, both genetic constructs for each GMR type, long and short, were used for the purpose of comparing levels of expression between *longGMR* and *shortGMR*. Graph shows *shortGMR* caused ~9-fold greater level of GFP reporter expression than *longGMR*.

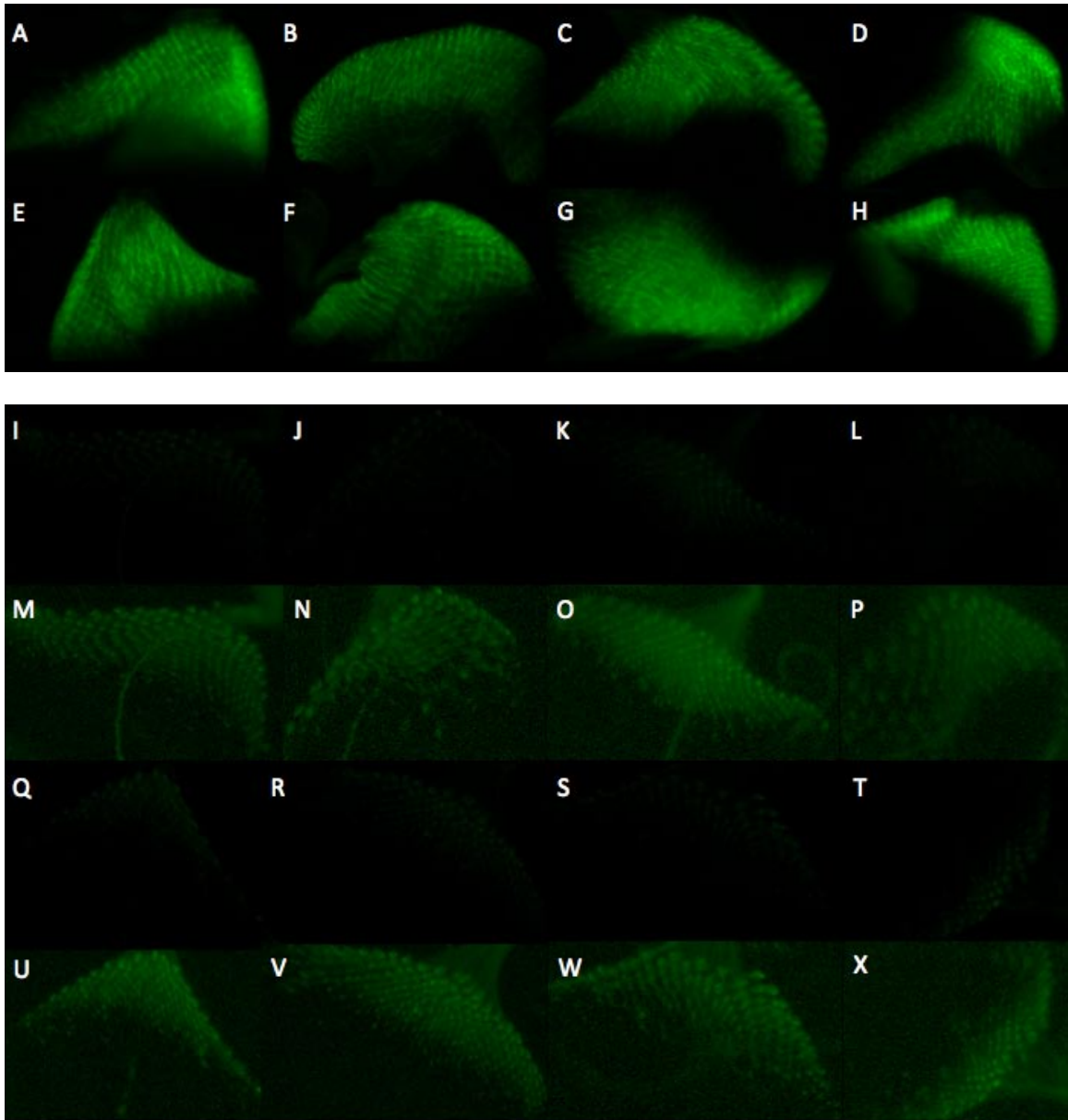


Figure 4. Representative fluorescence microscopy images of larval eye disc structures. A-D) Eye discs dissected from “sGMR” genotype. E-H) Eye discs dissected from “sGMR *Dikar*” genotype. There is no obvious difference in mean photon intensity between images A-D and images E-H, indicating no qualitative impact of *Dikar* expression on *sGMR*-driven expression of GFP reporter. I-L) Eye discs dissected from “lGMR” genotype. M-P) Corresponding digitally enhanced versions of I-L for the purpose of visualizing eye disc structures present in image. Q-T) Eye discs dissected

from “*lGMR Dikar*” genotype. U-X) Corresponding digitally enhanced versions of images Q-T for the purpose of visualizing eye disc structures present in image. Analogous to *sGMR*, there is no obvious difference in mean photon intensity between images I-L and images Q-T, indicating no qualitative impact of *Dikar* expression on *lGMR*-driven expression of GFP reporter.